Highly Selective Mechanism-Based Thrombin Inhibitors: Structures of Thrombin and Trypsin Inhibited with Rigid Peptidyl Aldehydes†

R. Krishnan,‡ E. Zhang,‡,§ K. Hakansson, R. K. Arni, and A. Tulinsky*

Department of Chemistry, Michigan State University, East Lansing, Michigan 48823

M. S. L. Lim-Wilby, O. E. Levy, J. E. Semple, and T. K. Brunck

Corvas International Inc., 3030 Science Park Road, San Diego, California 92121

Received April 14, 1998; Revised Manuscript Received June 10, 1998

ABSTRACT: The crystal structures of three highly potent and selective low-molecular weight rigid peptidyl aldehyde inhibitors complexed with thrombin have been determined and refined to *R* values 0.152−0.170 at 1.8−2.1 Å resolution. Since the selectivity of two of the inhibitors was >1600 with respect to trypsin, the structures of trypsin-inhibited complexes of these inhibitors were also determined ($R = 0.142-0.157$ at 1.9−2.1 Å resolution). The selectivity appears to reside in the inability of a benzenesulfonamide group to bind at the equivalent of the D-enantiomorphic S3 site of thrombin, which may be related to the lack of a 60-insertion loop in trypsin. All the inhibitors have a novel lactam moiety at the P3 position, while the two with greatest trypsin selectivity have a guanidinopiperidyl group at the P1 position that binds in the S1 specificity site. Differences in the binding constants of these inhibitors are correlated with their interactions with thrombin and trypsin. The kinetics of inhibition vary from slow to fast with thrombin and are fast in all cases with trypsin. The kinetics are examined in terms of the slow formation of a stable transition-state complex in a two-step mechanism. The structures of both thrombin and trypsin complexes show similar well-defined transition states in the S1 site and at the electrophilic carbon atom and Ser195OG. The trypsin structures, however, suggest that the first step in a two-step kinetic mechanism may involve formation of a weak transition-state complex, rather than binding dominated by the P2−P4 positions.

Thrombin is the terminal enzyme in the coagulation cascade, regardless of the nature of the triggering event (*1*). Its principal roles in blood clotting are the cleavage of fibrinogen to produce fibrin and the activation of circulating platelets, causing them to aggregate (*2*). Thrombin inhibitors currently in clinical use act indirectly, the heparins by activating the serpin antithrombin III and warfarin by inhibiting hepatic synthesis of thrombin and other vitamin K-dependent enzymes (*3*, *4*). A corollary of the indirect modes of action is that efficacy and safety are not optimal. Other strategies for inhibiting clot formation have recently been extensively reviewed (*5*); the most promising modes of inhibition, with the best possibilities of yielding orally bioavailable drugs and the most appropriate pharmacokinetic properties, involve the direct inhibition of thrombin and include the use of mechanism-based strategies (*6*, *7*).

Thrombin is a serine protease of the trypsin family, as are most of the other enzymes involved in hemostasis (*2*). Its selective inhibition has been a target of drug design and synthesis efforts for many groups (*8*). Trypsin-like enzymes unrelated to coagulation, but known to be necessary for normal physiological functions, may also be accidental targets of less selective inhibitors, causing potential adverse side effects; to further complicate the issue, there are probably additional important trypsin-like enzymes yet to be discovered. For this reason, trypsin, thought to be the most promiscuous of the enzymes in its family, has become the specificity marker for undesirable affinity (*9*, *10*), although inhibition of trypsin itself has not been shown to be deleterious to health (*11*).

We have previously reported the synthesis of highly potent and selective low-molecular weight (<600) thrombin inhibitors (*12*, *13*). The highest ratio of activities of human thrombin to bovine trypsin reported to date (>25000 for CVS1695, Figure 1) was achieved through excellent subnanomolar potency against thrombin and poor binding affinity for trypsin (Table 1). Kinetic measurements of the inhibition of thrombin and trypsin by three inhibitors (CVS1578, CVS1694, and CVS1695; Figure 1) showed considerable differences. All displayed fast kinetics with trypsin over the 1 h time course of measurement. In contrast, a gradation of rates of inhibition was observed with thrombin: fast with CVS1694, slow with CVS1695, and intermediate with CVS1578. Thus, the binding modes and interactions of the inhibitors with the two proteases loomed as important parameters for the future design of inhibitors with similar attributes.

The diastereomers CVS1694 and CVS1695 were made as a 1:1 mixture from a precursor racemic at the equivalent

† Supported by NIH Grant HL 43229 and Corvas International, Inc.
* To whom correspondence should be addressed.
‡ Contributed equally to the work.
§ Present address: Parke-Davis Pharmaceutical Research, 2800 Plymouth Rd., Ann Arbor, MI 48105.

S0006-2960(98)00840-X CCC: $15.00
Published on Web 08/08/1998

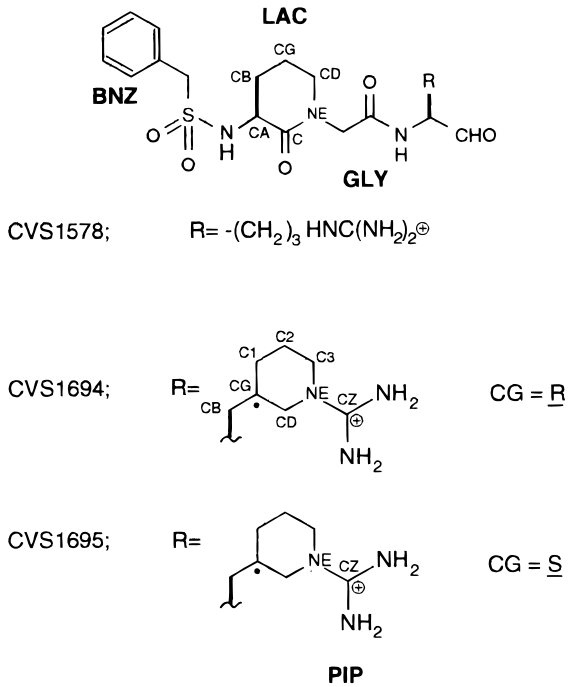

FIGURE 1: CVS inhibitors. The diastereomeric carbons of the piperidyl rings of CVS1694 and CVS1695 are designated with dots (CG atom).

Table 1: K_i Values, Kinetics, and Selectivity Ratios of CVS Inhibitors against Human Thrombin and Bovine Trypsin

	CVS1578	CVS1694	CVS1695
thrombin	1.0 nM (slow)	4.4 nM (fast)	0.32 nM (slow)
trypsin	190 nM (fast)	7300 nM (fast)	8100 nM (fast)
trypsin and/or thrombin	190	1600	25000

P1-CG position,[1] and resolved at the final stage of purification into two distinct compounds, each having significantly different activities with respect to thrombin and trypsin (Table 1). The absolute configurations of the two isomers, although critical for activity, were unassigned at this stage. In the preliminary report of the syntheses and binding affinities of the inhibitors, initial configuration assignments for CVS1694 and CVS1695 were made on the basis of the crystal structures of the thrombin complexes (*13*), which have now been confirmed unequivocally by more detailed analyses of the X-ray diffraction data sets.

Initially, it was anticipated that the bulky P1 guanidinopiperidyl group of CVS1694 or CVS1695 would bind with the hydrophobic trimethylene fragment of the ring facing inward in the S1 site of thrombin with minimal solvent exposure. It was also believed that the cognate binding of these compounds to trypsin would not be as facile due to the side chain of Ser190 in its S1 site, reducing both the hydrophobicity and size of the pocket relative to those of Ala190 of thrombin (*14*, *15*). Subsequent modeling, however, revealed that the P1 groups of both CVS1694 and CVS1695 would probably not fit in thrombin unless the three methylenes were turned toward the solvent so that the all-important salt bridge from the guanidino group to Asp189 could be made. It was thus unexpected that these inhibitors would exhibit such a difference in potency between the two enzymes. The X-ray crystal structures described herein help clarify the different binding modes of the enzymes and explain some, but not all, of the observed properties of the inhibitors.

[1] The nomenclature for inhibitor residues and enzyme sites follows that of Schlechter and Berger (*36*).

MATERIALS AND METHODS

Crystallization

CVS1578−Thrombin. A 1.0 mL sample of −80 °C frozen thrombin (1.06 mg/mL in 0.75 M NaC1) was thawed on ice with a 10-fold molar excess of hirugen.[2] The solution was then diluted with 1.0 mL of 0.1 M sodium phosphate (pH 7.3) and 1 mM NaN_3. A 10-fold molar excess of CVS1578 dissolved in 25 μL of methanol was added to the hirugen−thrombin solution, and the sample was concentrated to 0.25 mL in a refrigerated centrifuge with Centricon-10 concentrators. The active site-inhibited enzyme was incubated as hanging drops in a 1:1 mixture of the equilibrating solution [24% PEG 8000, 0.1 M phosphate buffer (pH 7.3), and 1 mM NaN_3]. Seeds of hirugen−thrombin crystals were added after equilibration for 24 h, and newly formed CVS1578−Throm ternary complex crystals were further enlarged by macroseeding (*16*, *17*).

CVS1694− and CVS1695−Thrombin. Binary complex hirugen−thrombin crystals suitable for X-ray analysis were prepared as described in earlier work (*16*, *17*). To one of these crystals in 4 μL of its storage solution [28% PEG 8000, 0.1 M Tris buffer (pH 7.5), 0.2 M sodium acetate, and 1 mM NaN_3] was added 1 μL of a storage solution containing 15 mM CVS1694 to give a 3 mM concentration of CVS1694 to form the ternary thrombin complex CVS1694−Throm. Seven hours later, 1 μL of the solution was removed and another 1 μL of the 15 mM CVS1694 solution was added. This procedure was repeated the next day to increase the concentration of CVS1694 to 7.3 mM in the drop, and it was then allowed to equilibrate for another 3 days. A similar soaking experiment was carried out with CVS1695 to produce ternary complex CVS1695−Throm crystals.

CVS1694− and CVS1695−Trypsin. Bovine trypsin (Sigma Chemical Co., St. Louis, MO) was dissolved in distilled water to make a 40 mg/mL protein solution. An 8.8 μL hanging drop was set up at room temperature by mixing 4 μL of protein solution and 4 μL of well solution [1.9 M $(NH_4)_2SO_4$, 0.1 M Tris buffer (pH 7.0), and 0.01 M $CaC1_2$] with 0.8 μL of 1.0 M benzamidine and the mixture equilibrated against 1.0 mL of well solution. Rod-shaped crystals that were enlarged by macroseeding in a pre-equilibrated hanging drop with a slightly lower concentration of $(NH_4)_2SO_4$ (1.8 M) appeared in about 4 days.

An enlarged crystal (1.1 mm × 0.5 mm × 0.5 mm) was washed three times by exchanging 50 μL sitting drops of a storage solution [2.5 M $(NH_4)_2SO_4$, 0.1 M Tris buffer (pH 7.0), and 0.01 M $CaC1_2$]. The storage solution was exchanged four more times in the next 5 days to further

[2] Abbreviations: hirugen, sulfated Tyr63-*N*-acetylhirudin 53−64; CVS1578−Throm, ternary complex of CVS1578, thrombin, and hirugen; CVS1694−Throm, ternary complex with CVS1694; CVS1695−Throm, ternary complex with CVS1695; CVS1694−Tryp, binary complex of CVS1694 with trypsin; CVS1695−Tryp, binary complex of CVS1695 with trypsin; PPACK, D-Phe-Pro-Arg-chloromethyl ketone; CVS1347, benzyl-SO_2-Met(O_2)-Pro-Arg(CO)OH.

Table 2: Crystal Data Collection and Structure Refinement Statistics and Parameters of the CVS Inhibitor Complexes

	thrombin			trypsin[a]	
CVS complex	1578	1694	1695	1694	1695
space group	*C*2	*C*2	*C*2	$P2_12_12_1$	$P2_12_12_1$
cell constants					
a (Å)	71.26	71.14	71.13	63.67	63.76
b (Å)	71.29	72.26	72.12	63.20	63.14
c (Å)	72.99	72.73	73.14	69.22	69.29
β (deg)	100.9	100.7	100.8	−	−
resolution (Å)	1.8	2.1	2.1	1.9	2.1
no. of observations	40769	36756	26856	41525	39107
R_{merge} (%)	7.3	5.9	5.2	4.3	4.3
R for the outermost shell (%)	18.4	13.7	9.1	10.3	6.1
outermost shell (Å)	2.0−1.8	2.4−2.1	2.3−2.1	2.0−1.9	2.3−2.1
no. of independent reflections	22257	19592	18157	16355	13609
redundancy	1.8	1.8	1.5	2.5	2.9
completeness (%)	61	86	79	72	76
outermost shell (%)	38	39	74	43	52
I/σ (outermost shell)	2.3	5.0	5.7	5.0	10.1
refinement					
no. of reflections	17478	17909	16839	15565	13035
$\langle\|F_o\|^2/\sigma\rangle$	2.0	1.5	1.5	2.0	1.5
range (Å)	7.0−1.8	7.0−2.1	7.0−2.1	9.0−1.9	9.0−2.1
no. of solvent molecules[b]	157	163	174	176	180
R value (%)	15.2	17.0	15.7	15.7	14.2
rms deviations					
bond lengths (Å)	0.018	0.012	0.012	0.015	0.015
bond angle distances (Å)	0.040	0.040	0.042	0.035	0.050
$\langle B\rangle$ (Å^2)	26.5	29.2	27.5	20.7	17.1
rms-B_{mc} (Å^2)[c]	1.9	1.5	1.8	1.5	1.4
rms-B_{sc} (Å^2)[c]	3.2	2.7	3.3	3.3	3.7

[a] Data collected at 4 °C. [b] Only water with an occupancy of >0.5. [c] rms deviation of the *B* factor of bonded atoms (mc, main chain; sc, side chains).

remove and minimize the concentration of benzamidine, which is noncovalently bound and dissociates from trypsin.

A 10 μL aliquot of the 50 μL storage solution containing the benzamidine-free crystal was removed, and 10 μL of a CVS1694 storage solution [0.02 M CVS1694, 2.5 M $(NH_4)_2SO_4$, 0.1 M Tris buffer (pH 7.0), and 0.01 M $CaC1_2$] was added to obtain a concentration of 5 mM CVS1694 to form the binary CVS1694−Tryp complex. The same procedure was repeated the next day, thereby increasing the concentration of CVS1694 to 8.75 mM. The crystal was then placed in the storage solution of 20 mM CVS1694 and equilibrated for an additional 2 days. The benzamidine back-soaking and the CVS1694 soaking experiments were completed in 9 days, and the crystal was mounted in a capillary for X-ray intensity data collection. Diffraction quality crystals of the CVS1695−Tryp complex were prepared using a similar procedure.

Intensity Data Collection

X-ray diffraction data were collected using a Rigaku R-AXIS II imaging plate detector and a Rigaku RU200 rotating anode X-ray source with a fine focus filament (0.3 mm × 3.0 mm) operating at 50 kV and 100 mA. The CVS1694−Tryp and CVS1695−Tryp data sets were measured similarly but with the aid of Molecular Structure Corp. focusing mirrors and at 4 °C. The thrombin complexes are isomorphous with respect to hirugen−thrombin crystals that are monoclinic, in space group *C*2, with one complex per asymmetric unit (Table 2) (*17*). The trypsin complex is isomorphous with respect to β-trypsin (*18*). The diffraction data of the complexes were processed to structure amplitudes and averaged using the Rigaku suite of programs. Some important data collection statistics and parameters are given in Table 2.

Structure Refinement

The structures of the active site- and fibrinogen recognition exosite-inhibited (hirugen) complexes of thrombin were refined starting with the coordinates of the hirugen−thrombin structure (PDB entry code 1HAH) (*19*), less hirugen. A rigid-body rotation−translation refinement was initially carried out to place the model structure more accurately in the unit cell of the thrombin complex. Restrained least-squares refinement with PROLSQ (*20*, *21*) at 2.8 Å resolution located the active site inhibitor and the hirugen molecule. Water molecules and two Na^+ ions (*22*, *23*) were introduced at 2.5 Å resolution. In the final stages of refinement, a Bragg angle-dependent $\sigma\langle|F_o|\rangle$ was used to weight the diffraction pattern based on $\langle|\Delta F|\rangle$ in different 2θ shells. The β-trypsin structure (PDB entry code 1TLD) (*18*) was used as a starting model, and refinement was carried out as above. A Ca^{2+} ion was located in the Ca-binding loop of trypsin at 2.5 Å resolution and included in calculations. Indicative refinement statistics and parameters of the structures are compared in Table 2. The coordinates of all five structures have been deposited with the Brookhaven Protein Data Bank: access numbers 1ba8 (CVS1578−Throm), 1bb0 (CVS1694−Throm), 1ca8 (CVS1695−Throm), 1zzz (CVS1694−Tryp), and 1yyy (CVS1695−Tryp).

Kinetic Parameters for Inhibition of Thrombin and Trypsin

The amidolytic activities of human α-thrombin (Enzyme Research Laboratories, South Bend, IN) and bovine trypsin

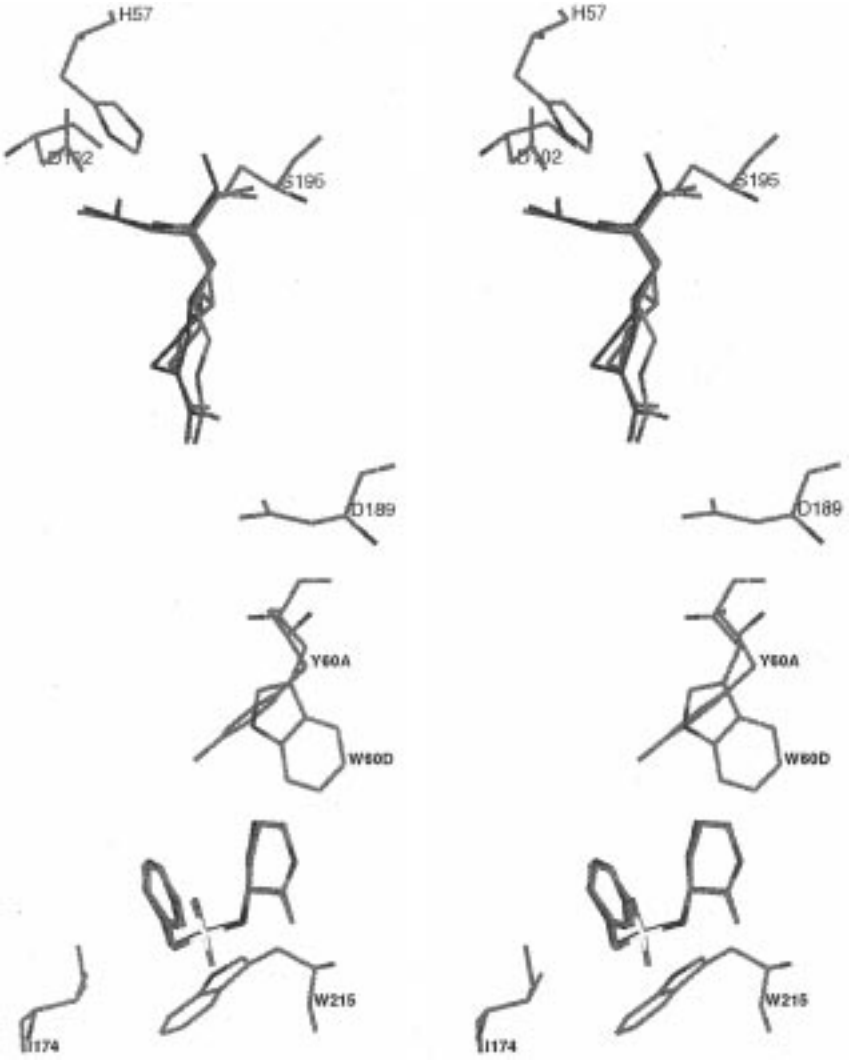

FIGURE 2: Stereoview of thrombin-bound CVS inhibitors. (a, top) S1 specificity and S2 subsite. For CVS1578, carbons are green, nitrogens blue, and oxygens red. CVS1694 is all red. CVS1695 is all blue. The background thrombin structure is that of CVS1578−Throm with atom colors like those for CVS1578. (b, bottom) Lactam and benzylsulfonamide. Lactam between S2 and D-enantiomorphic S3 subsites, benzylsulfonamide in the latter site with sulfur (yellow), and thrombin as in part a.

(Worthington, Freehold, NJ) were measured as the rates of cleavage of Pefachrome tPA (Pentapharm, Basel, Switzerland) and S-2222 (Chromogenix, Franklin, OH), respectively, at ambient temperature (22−25 °C) in 96-well Microtiter plates (Dynatech, Chantilly, VA). The increase in absorbance on production of the chromophore *p*-nitroaniline at 405 nm was monitored in triplicate using a ThermoMax kinetic microplate reader (Molecular Devices, Sunnyvale, CA). In all cases, the buffer used was 10 mM HEPES (pH 7.5), 150 mM NaCl, and 0.1% bovine serum albumin.

The inhibitory potency of a compound was first estimated by its IC_{50}, the concentration of inhibitor required to halve the activity of the enzyme in the absence of the inhibitor. The reactions were initiated by the addition of substrate to the well, with and without preincubation of the inhibitor with enzyme for 30 min. The final concentrations of reactants in a total volume of 200 μL were 0.5 nM enzyme and 250 μM Pefachrome tPA or S-2222. The kinetics of inhibition were considered slow when the ratio of IC_{50} values (no incubation/incubatum) exceeded 10-fold. For the determination of the equilibrium dissociation rate constant, K_i, for "slow tight-binding" inhibitors of thrombin, the reaction was initiated by addition of 0.2 nM enzyme to the wells containing 750 μM substrate. The IC_{50} and K_i were derived from 10 initial velocity and 18−22 progress curves, respectively, as previously described (*12*, *24*).

RESULTS

All three inhibitors bind to thrombin similarly (Figure 2) in an extended conformation comparable to substrate (*25*, *26*) and the archetypical inhibitor PPACK (*14*). The positioning of the arginyl atoms of CVS1578 in the specificity S1 site closely overlaps the guanidino group and two of the atoms of the piperidyl rings of bound CVS1694 and CVS1695 (Figure 2a); the hydrophobic $(CH_2)_3$ loop of the piperidyl protrudes out of the elongated S1 pocket toward the solvent region. The diastereoisomeric configurations at the CG atoms of CVS1694 and CVS1695 (Figure 2a) have been identified to be *R* and *S*, respectively, while the piperidyl rings have approximate chair and boat conformations, respectively. Two of the inhibitors (CVS1578 and CVS1695) make identical doubly hydrogen-bonded salt bridges with Asp189 of thrombin, while one distance is longer in CVS1694 (Table 3). In addition, the locations of the lactam rings in the S2 subsite of all three and the benzyl groups of the benzylsulfonylamide in the D-enantiomorphic S3 aro-

Table 3: Active Site Hydrogen Bonds of CVS Inhibitors[a]

		thrombin			trypsin	
		CVS1578	CVS1694	CVS1695	CVS1694	CVS1695
(A) Guanidino Interactions						
PipNHA[b]	Asp189OD1	2.9	2.9	2.8	2.9	2.8
PipNHB	Asp189OD2	3.1	(3.3)	3.0	(3.4)	(3.3)
PipNHA	Gly219O	2.9	(3.2)	3.1	2.9	2.8
PipNHB	O_w414/407/407[c]	3.0	2.7	2.9	–	–
PipNHB	O_w412	–	–	–	2.9	3.0
O_w414/407/407	Phe227O	3.0	2.9	2.9	–	–
O_w412	Val227O	–	–	–	2.9	2.9
ArgNE	O_w455	2.9	–	–	–	–
O_w455	Gly219O	2.6	–	–	–	–
O_w455	O_w497	2.7	–	–	–	–
PipNHA	O_w434	–	–	–	2.8	2.6
(B) Antiparallel β-Strand Interactions						
PipN	Ser214O	3.0	3.1	3.1	2.7	2.6
GlyO	Ow519/459/459[c]	(3.3)	2.8	2.7	–	–
LacO	Gly216N	(3.4)	(3.3)	(3.3)	3.0	3.0
LacN	Gly216O	(3.2)	(3.2)	3.0	2.5	2.5
SO_2O	Gly218N	–	–	–	2.9	2.9

[a] Distances greater than 3.0−3.1 Å (in parentheses) possibly not hydrogen bonds. [b] Pip is Arg in CVS1578. [c] Water numbers correspond to the respective thrombin complexes.

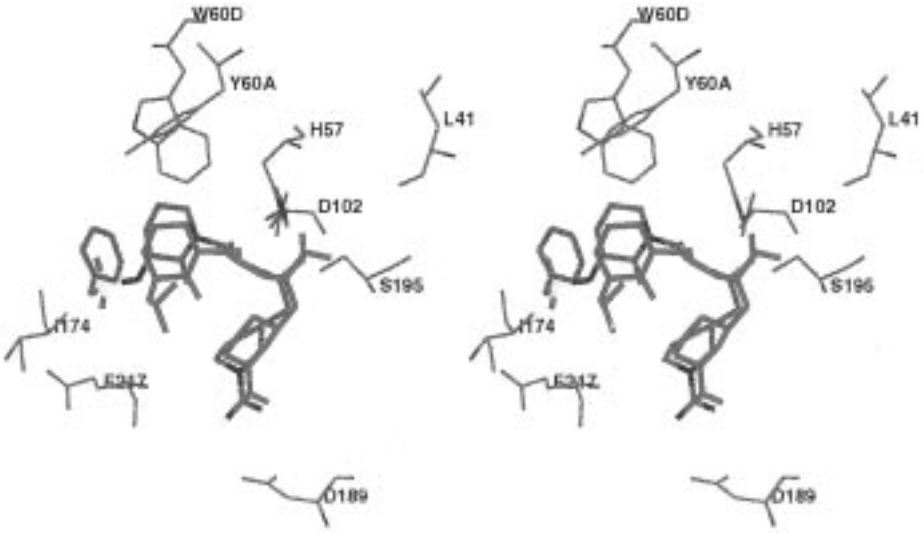

FIGURE 3: Stereoview of the superposition of the active sites of CVS1695−Throm and CVS1695−Tryp. The atoms of CVS1695−Throm are colored as described previously, with CVS1695 being bold and the CVS1695 of CVS1695−Tryp red.

matic site are isostructural (Figure 2b) and the sulfonyl linker is exposed at the surface of thrombin in contact with the solvent.

The similarity of the three inhibitors does not appear to apply to the interactions of their aldehydic carbonyl oxygen atoms (Figure 2a). Although the electrophilic carbon atom is well-defined in electron density and in a normal transition-state stance, the position of the oxygen was difficult to fix with certainty. It appears to hydrogen bond with Gly193N and Ser195N of the oxyanion hole in CVS1578 and CVS1694 (*27*−*29*), but in CVS1695, it makes a hydrogen bond with His57NE of the catalytic triad like the α-ketoacid inhibitor CVS1347 (*24*). In all three cases, however, the alternate orientation cannot be completely ruled out if occupancy between the two positions is more or less equally distributed.

Whereas the K_i values of CVS1694 and CVS1695 for thrombin are in the lower nanomolar range, the values for trypsin are only about 7−8 μM (Table 1). Consequently, partial inhibitor occupancy, much higher inhibitor *B* values, or the lack of a transition-state conformation might be expected with the trypsin complexes. The electron density of the bound piperidyl and lactam rings of the CVS1694 and CVS1695 inhibitors in the S1 and S2 sites of trypsin defines the two rings clearly. There is no density, however, corresponding to the benzyl groups of each inhibitor in either enantiomorphic S3 subsite. The density for the sulfoxide groups projects to the surface differently from the thrombin complexes and in a manner implying that the benzyl groups are disordered in the adjoining solvent space. The net result of the latter is a displacement of the lactam rings in the trypsin complexes from their position in thrombin (Figure 3). These latter differences in structure between the thrombin and trypsin complexes must be the sources of the major underlying contributions that produce the 25000-fold difference in selectivity observed between the two enzymes (Table 1).

To distinguish between large *B* values for the inhibitors in the trypsin complexes and partial occupancy, an attempt was made to approximate the occupancy of the inhibitors in

the following manner. The occupancy of the inhibitor was set at 0.75, and the *B* values were fixed at a constant 25 Å^2. Three cycles of occupancy refinement, keeping the *B* values of the inhibitor constant, followed by two cycles of inhibitor and protein *B* refinement, keeping the occupancies constant, were carried out. Surprisingly, the occupancies of the guanidinopiperidyl group and the remainder of the P1 residue in both inhibitors increased to near unit values with *B* values remaining at about 25 Å^2, while the occupancies of the P2 glycine (0.80), the P3 lactam (0.66), and the sulfonyl group (0.48) decreased uniformly from the P1 position to the flexibly and/or statically disordered benzyl group; the *B* values also increased but not to values of 40−50 Å^2 as observed with the unit occupancy inhibitor.[3] The analysis suggests that the inhibitors do indeed occupy trypsin nearly fully, but that the binding is much more tenuous away from the S1 specificity site. This is also consistent with the 20 mM concentration of inhibitor used in the soaking solution to form the complex, which is about a 1000-fold excess compared to that for the protein in a single crystal, thus shifting the equilibrium favorably toward the bound state.

The $2F_o - F_c$ and $F_o - F_c$ electron densities in the S1 specificity site of CVS1695−Tryp both showed a characteristic bend similar to that observed in thrombin for the *S*-diastereomer, boat conformation of CVS1695. A fairly straight (unbent) density was observed in CVS1694−Tryp like that for the chair conformation of the *R*-stereoisomer of thrombin. However, both inhibitor configurations and/or conformations (*S*-boat and *R*-chair) refined equally well against both CVS1694−Tryp and CVS1695−Tryp X-ray diffraction data sets (*R* values did not change significantly). The same, however, did not apply to the thrombin complexes. The most likely reason for the ambiguity with the trypsin complexes is that the inhibitor contribution to diffraction is relatively weak compared to that of the trypsin molecule and its highly ordered surrounding solvent water structure. Therefore, the stereochemistry and the ring conformation of the trypsin-bound inhibitors have been basically inferred from the structures of the thrombin complexes. Conversely, while the aldehyde group of the inhibitors hinted at diversity in orientation in the thrombin structures, both trypsin structures showed the carbonyl oxygen atom unambiguously making hydrogen bonds in the oxyanion hole.

DISCUSSION

Thrombin Complexes

S1 Specificity Site. The atoms of the thrombin-bound guanidinopiperidyl groups of CVS1694 and CVS1695 that can correspond to an arginyl group closely mimic the positions of the arginyl atoms of thrombin-bound CVS1578 (Figure 2a). The largest deviations are 0.7, 0.6, and 0.4 Å between CD, NE, and CZ (Figure 1). In two cases (CVS1578 and CVS1695), the guanidinium groups make symmetrical doubly hydrogen-bonded salt bridges with Asp189 of thrombin. One of the hydrogen bonds is longer and thus questionable in CVS1694−Throm (Table 3). The CVS1578 inhibitor displays the ligand−water−protein hydrogen bonding interactions that appear to be conserved and common to thrombin-bound arginyl groups (*23*, *30*), except that Glu192 does not hydrogen bond with O_w455, the water molecule which is hydrogen bonded to NE of the arginyl of CVS1578, while the heterocyclic NE atom of CVS1694 or CVS1695 has no water-stabilizing interaction (Table 3). The Glu192 residue in CVS1578−Throm is in a rare up conformation for an active site arginyl-occupied thrombin rather than in the down orientation shielding the S1 pocket and the arginyl group from bulk solvent (*19*). However, O_w455 hydrogen bonds further with Gly219O and O_w497.

The piperidyl inhibitors also generally display the same conserved ligand−water−protein hydrogen bonding interactions but with displacements and differences. Most noteworthy is the above-mentioned water molecule that hydrogen bonds to NE of the guanidinium group, absent probably because of the less basic piperidyl ring nitrogen atom. Along with the missing water molecule, most of the Glu192 side chain of thrombin is flexible and orientationally disordered in both piperidyl inhibitor complexes. This could be partially due to the bulky hydrophobic $(CH_2)_3$ loop of the piperidyl ring protruding out along the surface of the S1 pocket, thereby interfering with the otherwise stabilizing protection of Glu192. The one largest difference between the arginyl and piperidyl groups in the S1 site of thrombin is thus the guanidino NE atom interaction and its accompanying water-mediated hydrogen bonds (Table 3). An additional, lesser difference could be the marginally longer PipNHB−Asp189OD2 distance (3.3 Å) in the CVS1694 complex. This, however, should not be expected to diminish the energy of the salt bridge interaction in the specificity site to any great extent. Since the antiparallel β-strand in the active site between the inhibitor and thrombin is comparable for all three inhibitors (Table 3), the decrease in binding from CVS1578 to CVS1694 by about a factor of 4 (Table 1) must reside in the loss of the guanidino NE atom interaction and associated water-mediated hydrogen bonds.

Although it is possible for the piperidyl groups to assume a number of different boat and chair conformers with respect to the diastereoisomeric (*R*,*S*) center (CG carbon atom), the planarity requirement of the ring nitrogen, the all-important salt bridge interaction with Asp189 in the S1 subsite, and the virtually identical inhibitor binding modes in the S2 and S3 sites of thrombin (Figure 2b) appear to limit the conformational choices to an overall similarity in binding (Figure 2a). The guanidinium groups and an accompanying ring CD carbon atom are closely isostructural in CVS1694− and CVS1695−Throm, while seven atoms of the guanidinopiperidyl ring mimic the arginyl group of CVS1578−Throm (Figure 2a). This likeness, without doubt, is the primary force of the diastereoisomeric binding interaction, which also strongly influences the boat or chair conformational choice of the diastereomers. The overall similarity in binding between the two piperidyl inhibitors is achieved with CG of CVS1694−Throm in an *R*-configuration, the ring in a chair conformation with the CB−CG bond equatorial; in CVS1695−Throm, these three are *S*, boat, and equatorial, respectively. The analogous binding in the S1 specificity pocket is primarily due to the combination of the *R*- and *S*-configurations and an interesting relationship between the boat and chair conformers of the inhibitors; both are joined to CB equatorially, through an apical atom in the boat but

[3] A *B* value of 50 Å^2 was set to be the maximum allowable *B* value during refinement; any *B* factors calculated to be >50 Å^2 were automatically set to the maximum value of 50 Å^2.

through a planar nonapical atom of the chair. The boat and chair conformations, however, are somewhat twisted and so are at best only approximate due to bond angle distortions (up to 7−8°). The same applies to the bond angles around the diastereomeric centers, which render the assignment of the *R*- and *S*-configurations a little less obvious and definite. Gas phase electron diffraction studies reveal deviations of 5−7° from ideality for the chair form of cyclohexane (*31*), so even greater deviations are to be expected in crowding a piperidyl ring into the specificity pocket of thrombin, presumably evolved for arginine. The cogent observation here is that the guanidinopiperidyl groups do not fit into the specificity site of thrombin without small distortions. In the end, the *R*- and *S*-diastereomers do so in different ways but resemble one another and mimic arginine.

The $\langle B \rangle$ values of the CVS1694 (36 Å^2) and CVS1695 (29 Å^2) inhibitors determined for the refined structures bound to thrombin correlate with their K_i values (Table 1). Whereas the *B* values of the CVS1695 inhibitor are comparable to the average *B* of thrombin (Table 2), those of CVS1694 are about 25% larger. This may be a manifestation of the factor of 14 between the K_i values of CVS1694 and CVS1695 (Table 1) but is not the cause of the difference. The *B* values of the two contrast markedly with that of CVS1578 (16 Å^2), which is about half the average of thrombin in the inhibitor complex (Table 2), consistent with the high degree of specificity of the S1 site of thrombin for an arginyl side group. Examining the $2F_o - F_c$ inhibitor electron density maps of CVS1694 and CVS1695 at higher contour levels (2.0−2.5σ) correlates closely with the foregoing; the maps only display density in the S1 site that corresponds to the comparable arginyl atoms of the guanidinopiperidyl group with the remaining density of the $(CH_2)_3$ loop of the ring (C1, C2, and C3; Figure 1) below this contour level. That the *R*- and *S*-diastereomers are structurally different, but resemble each other in their bound conformations, suggests that the factor of 14 between their binding affinities must be due to other sources. The interactions in the specificity site (Table 3) indicate only that CVS1694 may possibly not form a second hydrogen bond in the salt bridge with Asp189. As previously mentioned, the salt bridge remains intact and the remainder of the binding is very similar to that of CVS1695, so it is difficult to account for the difference of 14 in their binding affinities.

Aldehyde Group of the Inhibitors. The aldehyde group of the inhibitors appears to bind in two different conformations with thrombin. In CVS1694−Throm, the carbonyl oxygen atom is in the oxyanion hole hydrogen bonding with Gly193N and Ser195N, whereas in CVS1695−Throm, the oxygen atom hydrogen bonds with His57NE. The latter conformation also brings the carbonyl oxygen atom close (3.2 Å) to a water molecule (O_w527) that hydrogen bonds with Leu41O and is near Gly193N (3.3 Å). The two conformations differ in torsion angle around the carbon atom by about 180° with Ser195OG roughly orthogonal to the plane of the aldehyde group in both. The bond angles around the carbonyl carbon in either orientation do not suggest a tetrahedral intermediate, contrary to the short inhibitor CA−Ser195OG distance (1.7−1.9 Å). A consequence of the latter is several close single torsion contacts involving the carbonyl oxygen.

The positioning of the carbonyl oxygen atom is not clear in any of the $2F_o - F_c$ electron density maps of the inhibitors. Examining $F_o - F_c$ difference maps in the final stages of refinement, which did not include the aldehyde group in structure factor calculations through a series of refinement cycles, showed fairly convincing positive density at the 2σ level for either one or the other of the two above conformations. Since the significance of the density bordered on that of a half-occupancy water molecule (Table 2), the possibility of partial occupancy and both conformations being in the same structure could not be completely ruled out. The two conformations may be related to the protonization state of the imidazole of His57 (*24*). When the carbonyl oxygen is hydrogen bonded in the oxyanion hole, analogous to that of the PPACK−Throm (*14*) and other similar structures (*27*−*29*), His57 acts as a nucleophile and is not protonated. When the carbonyl oxygen is hydrogen bonded to His57NE, the imidazole is an electrophile and therefore must be protonated and have a positive charge. The crystals of both complexes were grown close to neutral pH. Since the p*K* value of histidine is in this range, the degree of protonization will depend on the exact pH of the mother liquor of the crystals. Unfortunately, the pH of the soaking solutions of the complexes was not measured per se, and only the pH of the buffered crystallization solutions is reported here.

Since the carbonyl oxygen atoms of CVS1578 and CVS1694 have the same orientation, the lack of a piperidyl NE interaction and resulting water-mediated structure in CVS1694−Throm (Table 3) remains the only apparent source for their difference in binding affinity (Table 1). The difference is surprisingly small considering that the difference in binding between an arginyl and lysyl residue at the S1 site of thrombin is about 2 orders of magnitude in favor of the former (*30*). However, the salt bridge in the S1 site of the lysyl case is not directly hydrogen bonded with Asp189 but, rather, is mediated by a water molecule. The much smaller difference in binding between CVS1578 and CVS1694 could be related to the ability of the piperidyl inhibitors to satisfactorily mimic the carbon backbone of an arginyl and, even more importantly, its doubly hydrogen-bonded salt bridge. The factor of 14 in binding between CVS1694 and CVS1695 (Table 1) could result from the positioning of the carbonyl oxygen atom of the inhibitors in the catalytic site of thrombin. Other differences between these two are the water-mediated hydrogen bond to Leu41O from the carbonyl oxygen in CVS1695 and the long 3.3 Å hydrogen bond with Asp189OD2 in CVS1694. Assigning the difference in binding to these relatively minor factors would not seem justified, unless the importance of the interaction with the catalytic site histidine has been grossly underestimated. The real enigma, however, is that CVS1578, with a P1 arginyl, binds to thrombin more than 3 times less effectively than CVS1695 (Table 1) with its bulky guanidinopiperidyl P1 group.

P2 Glycine Residue. This residue of the inhibitors does not make many contacts of <3.5 Å with thrombin except for a hydrogen bond from the carbonyl oxygen to a water molecule (Table 3). However, the carbonyl carbon and the CA atoms make three to five contacts of <4.0 Å with the imidazole ring of His57.

Lactam Ring. The main chain of all three inhibitors makes three antiparallel β-strand hydrogen bonds with the Ser214−

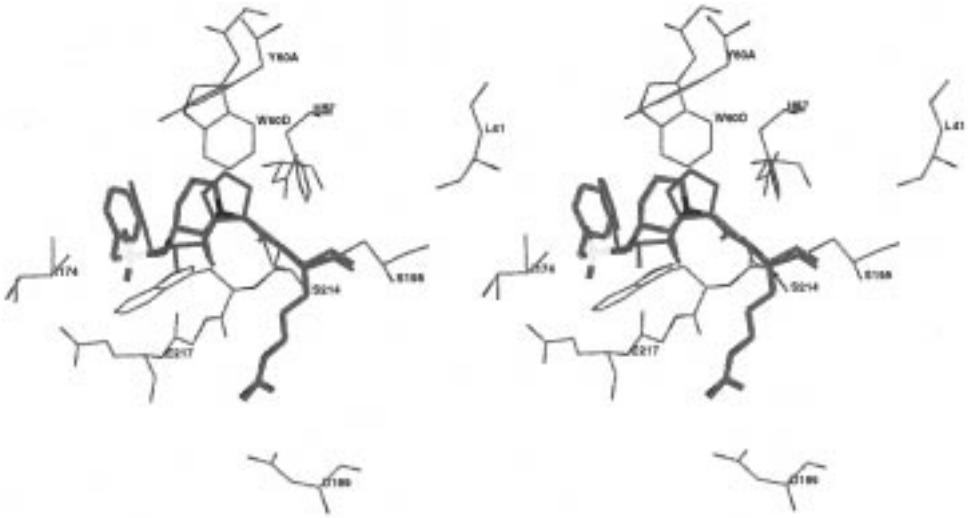

FIGURE 4: Stereoview of the superposition of the active sites of CVS1578−Throm and PPACK−Throm. The atoms of CVS1578 are colored as described previously, with CVS1578 being bold and PPACK of PPACK−Throm red.

Gly216 stretch of thrombin (Table 3). In CVS1578, LacO of the lactam ring additionally hydrogen bonds to O_w505, which is linked to the ArgNE atom of the inhibitor through O_w528 and O_w455. Such a water-mediated interaction is not observed with the ring nitrogen of the piperidyl groups of CVS1694 and CVS1695. In addition, one oxygen atom of the sulfonyl group is bridged to Gly219N by water-mediated hydrogen bonds. Thus, the peptide backbone of the inhibitors is held firmly in an extended conformation in the thrombin-bound structures.

The β-strand hydrogen bond distances of all three thrombin inhibitors appear to be stretched and on the long side (Table 3) as is generally common for thrombin and substrate-like active site inhibitors. Since none of the three thrombin−inhibitor β-strands are any more ideal than another, there is little or no difference to possibly account for binding differences. It is noteworthy, however, that the hydrogen bonds of the β-strand of the trypsin complexes are quite ideal and cooperatively suggest tighter binding (Table 3). The observation, however, is not consistent with the binding constants (Table 1).

The six-membered lactam ring at the P3 position of the inhibitors displays a half-chair-like conformation (Figure 2b). The lactam NE atom also corresponds to the glycyl amido nitrogen and is about 0.5−0.8 Å from the proline nitrogen position in P2 proline-bound inhibitors and/or substrates of thrombin (Figure 4) (*14*, *27*, *28*, *32*). The lactam ring does not overlap the bound proline structure but is displaced N-terminal to it by about 1.5−2.0 Å. The CB and CG atoms of the lactam ring make important hydrophobic van der Waals interactions with the tyrosyl and indole rings of Tyr60A and Trp60D of the 60-insertion loop of thrombin (Figures 3 and 4 and Table 4).

Benzylsulfonamide Group. It has been mentioned that the nitrogen of the benzylsulfonylamide is involved in an antiparallel β-strand hydrogen bond with thrombin (Table 3). Moreover, the benzylsulfonylamide superimposes closely on the same group of thrombin-bound CVS1347 (*24*), which has an L-methionyl residue at P3 and a proline instead of glycine at P2, as is present in CVS1694 and CVS1695. The sulfonyl group is located on the surface of thrombin, just beyond the entrance to the D-enantiomer S3 site, with one oxygen involved in water-mediated interactions. The benzyl group curls and back-tracks (Figures 3 and 4) and makes numerous hydrophobic interactions with thrombin residues Asn98, Leu99, Ile174, and Trp215 of the D-S3 binding site. The edge of the benzyl ring in particular approaches the face of the indole of Trp215 in a fashion typical of aromatic−aromatic interactions in proteins. Although there are no particularly close contacts, the Tyr60A−Trp60D segment of the 60-insertion loop forms a hydrophobic wall and closes off the D-enantiomorphic S3 aromatic binding pocket on one side. The displacement of the benzylsulfonamide by virtue of the P2 glycine residue (Figure 4) allows it to readily enter and occupy the D-S3 site, which might otherwise be difficult to achieve. The P2 positions, GlyCA in CVS1578 and ProCA in PPACK, are 0.85 Å apart with GlyN−ProN offset by 1.1 Å. The shift may be related to the absence of an α-substitution in CVS1578 permitting it to come closer to His57.

Table 4: van der Waals Contacts of <4.0 Å of the Lactam Group in Inhibitor−Thrombin Complexes

		CVS1578	CVS1694	CVS1695
LacCG	Tyr60ACE2	3.8	3.7	3.8
LacCG	Tyr60ACZ	3.7	3.7	3.7
LacCG	Tyr60AOH	3.5	3.5	3.5
LacCB	Trp60DCZ2	3.9	3.9	3.9
LacCG	Trp60DCZ2	3.5	3.4	3.7
LacCB	Trp60DCH2	3.9	3.9	3.9
LacCG	Trp60DCH2	3.4	3.6	3.8
LacCD	Trp60DCH2	−	3.9	−

Trypsin Complexes

The trypsin structures of CVS1694− and CVS1695−Tryp are generally more accurate than the corresponding ones of thrombin with respect to definition and clarity of electron density, atomic resolution, and $\langle B \rangle$ values (Table 2), but the inhibitors are not nearly as well-defined as those bound to thrombin. There is no $2F_o - F_c$ or $F_o - F_c$ electron density corresponding to the benzyl group of both inhibitors with trypsin; the density for the sulfonyl is weak in both cases, and the *B* values of the inhibitors increase progressively from the P1 guanidinopiperidyl group to the P3 lactam residue

(from about 30 to 50 Å^2). These values are to be compared to $\langle B \rangle$ values of 20 and 17 Å^2 for the trypsin molecule in CVS1694−Tryp and CVS1695−Tryp, respectively. A similar increasing trend, but not nearly as severe, was observed with the *B* values of the bound CVS1578 inhibitor in thrombin (from 14 to 26 Å^2), while those of the other two thrombin-bound inhibitors were essentially constant ($\langle B \rangle$ = 36 and 29 Å^2 for CVS1694 and CVS1695, respectively). The increasing individual *B* factor trend in CVS1578 is very well-defined due to more accurate *B* values resulting from higher resolution (1.8 vs 2.1 Å) and probably due to the presence of the ideally tight binding P1 arginyl rather than the more bulky piperidyl group.

Whereas the guanidinium groups of the piperidyl rings make symmetrical doubly hydrogen bonding salt bridges with Asp189 of thrombin, in both trypsin complexes, one of the distances is significantly longer (Table 3). However, this guanidino nitrogen atom is linked to Val227O through water-mediated hydrogen bonds (O_w412). The difference appears to be real and may reflect the small difference in the composition of the S1 binding site between the two enzymes (Ala190 in thrombin and Ser190 in trypsin). An earlier report described the design of a selective thrombin inhibitor with a bulky indole side chain at P1 that imparted trypsin selectivity. This was ascribed to unfavorable electrostatic interactions with Ser190 in trypsin and energy required to deform a slightly smaller specificity pocket of trypsin to accommodate the indole (*15*). Although the difference in the binding site can lead to overcrowding and nonbeneficial effects, the bulky side chain itself can be detrimental to binding even with the smaller Ala190 present.

The P1 and P2 positions of the trypsin-bound structures can be closely superimposed on the thrombin structures. The P3 lactam ring is an exception and is displaced from the equivalent position in thrombin (Figure 3). This is most probably due to the lack of the 60-insertion loop in trypsin, particularly the hydrophobic Tyr60A−Trp60D segment, which in thrombin interacts directly with the lactam (Table 4) and indirectly with the benzyl groups of the inhibitors. A beneficial effect of the movement of the lactam is production of a more ideal β-strand between inhibitor and Ser214−Gly216 of trypsin (Table 3). This shift, however, makes the placement of the benzyl group into the D-enantiomorphic S3 site practically impossible.

Since the guanidinopiperidyl groups bind similarly in the S1 specificity site of thrombin and trypsin, and differences begin to appear for the glycine and lactam residues in the S2 and S3 sites, the spectacular selectivity of 25 000 (Table 1) between thrombin and trypsin must be due to the lack of binding of the benzyl group in the D-enantiomorphic S3 subsite. Comparing this region in thrombin and trypsin shows only that Ile174 is a glutamine in trypsin, which does not seem to be enough of a change to account for the weak binding in trypsin. The conspicuous absence of the nearby thrombin 60-insertion loop in trypsin surfaces as the major factor for the lack of binding in this region. It has already been indicated that the lactam and benzyl rings interact with the insertion loop in thrombin (Table 4), which holds the segment of the inhibitor firmly. This is not the case with trypsin, where the electron density decreases and flexibility increases as the N terminus of the inhibitors is approached. The *B* values of the trypsin-bound inhibitors, which increase to the lactam, also support the conjecture. The position of the sulfonyl in trypsin (Figure 3) clearly indicates that the benzyl group is not in the D-enantiomorphic S3 site but projects off the surface of trypsin into solvent space in the crystals.

Kinetics of Inhibition

By conventional definition (*33*), CVS1578 and CVS1695 are slow-binding inhibitors of thrombin and fast inhibitors of trypsin. Fast inhibition of both thrombin and trypsin was observed for CVS1694 (Table 1). The definition of slow is operational and is applied to inhibitors whose extent of inhibition changes on a time scale of seconds to minutes, the scale of usual enzyme assays. Slow-binding inhibition is generally associated with compounds that mimic transition states or reactive intermediates of an enzymatic reaction (*34*), and many possible origins of slow kinetics have been proposed.

In the case of aldehyde inhibitors of serine proteases, at least two possible causes of the observed slow binding are evident. Arginine aldehydes (as CVS1578) are known to exist in four interconverting forms in water: the aldehyde (1−2%), the hydrate (30−40%), and two diastereomeric cyclic aminals (50−60%). The rigid arginine mimetics (as CVS1694 and CVS1695) show only hydrate and aldehyde forms in water. Apparent slowness could be ascribed to the low relative concentration of the aldehyde form, if this is the form that binds to the enzyme. Slowness of an aldehyde inhibitor could also be due to a slow conversion of an initial enzyme−inhibitor complex to a stable, transition-state complex in a two-step kinetic mechanism that has been observed directly for α-ketoamide thrombin inhibitors (*35*).

Since all three inhibitors exist in multiple forms in solution, it is difficult to assign the slowness of thrombin inhibition to interconversion of forms or low aldehyde concentration, when CVS1694 appears fast. Additionally, all three compounds are fast inhibitors of trypsin. A more likely explanation of the observations is the slow formation of a stable transition-state complex in a two-step mechanism. After days of equilibration during crystallization or crystal soaking, the structures of both thrombin and trypsin complexes for all the inhibitors show similar, well-defined inhibitor conformations in the S1 site and similar interactions between the electrophilic carbon atom and Ser195OG indicative of a transition-state complex. Even more interesting is the nearly identical binding of CVS1694 (fast) and CVS1695 (slow) to thrombin, thus revealing little about the origin of the kinetic differences. The trypsin structures, however, suggest the possibility that the first step in a two-step kinetic mechanism might involve formation of a weak transition-state complex, rather than binding dominated by P2−P4 (*35*). Indeed, the mechanism of inhibition by transition-state analogues might be rather more complicated with two kinetically fast steps operating simultaneously, one involving weak transition-state complex formation and one dominated by the binding of P2−P4. Either one or both of these weak and/or fast complexes could subsequently form the same fully bound enzyme−inhibitor complex in a slow step.

ACKNOWLEDGMENT

We thank Peter Bergum and Suzanne M. Anderson for the kinetic studies and Ruth F. Nutt and William C. Ripka

for useful discussions. We also thank Beisong Cheng and Igor Mochalkin for growing and preparing the trypsin complexed crystals and their intensity data collection, respectively.

REFERENCES

1. Rapaport, S. I., and Rao, L. V. M. (1992) *Arterioscler. Thromb. 12*, 1111−1121.
2. Colman, R. N., Marder, V. J., Salzman, E. W., and Hirsh, J. (1994) in *Hemostasis and Thrombosis: Basic Principles and Clinical Practice* (Colman, R. W., Hirsh, J., Lippincott, J. B., Marder, V. J., and Salzman, E. W., Eds.) 3rd ed., pp 3−18, J. B. Lippincott Co., Philadelphia, PA.
3. Hirsh, J., and Fuster, V. (1994) *Circulation 89*, 1449−1468.
4. Hirsh, J., and Fuster, V. (1994) *Circulation 89*, 1469−1480.
5. Ripka, W. C., and Vlasuk, G. P. (1997) *Annu. Rep. Med. Chem. 32*, 71−89.
6. Tapparelli, C., Metternich, R., Ehrhardt, C., and Cook, N. S. (1993) *Trends Pharm. Sci. 14*, 366−376.
7. Das, J., and Kimball, S. D. (1995) *Bioorg. Med. Chem. 3*, 999−1007.
8. Balasubramanian, B. N., Ed. (1995) Advances in the Design and Development of Thrombin Inhibitors, *Bioorganic Medicinal Chemistry*, Vol. 3, pp 999−1156.
9. Hilpert, K., Ackermann, J., Banner, D. W., Gast, A., Gubernator, K., Hadvary, P., Labler, L., Muller, K., Schmid, G., Tschopp, T. B., and van de Waterbeemd, H. (1994) *J. Med. Chem. 37*, 3889−3901.
10. Obst, U., Banner, D. W., Weber, L., and Diederich, F. (1997) *Chem. Biol. 4*, 287−295.
11. Flavin, D. F. (1982) *Vet. Hum. Toxicol. 24*, 25−28.
12. Semple, J. E., Rowley, D. C., Brunck, T. K., Ha-Uong, T., Minami, N. K., Owens, T. D., Tamura, S. Y., Goldman, E. A., Siev, D. V., Ardecky, R. J., Carpenter, S. H., Ge, Y., Richard, B. M., Nolan, T. G., Hakansson, K., Tulinsky, A., Nutt, R. F., and Ripka, W. C. (1996) *J. Med. Chem. 39*, 4531−4535.
13. Levy, O. E., Semple, J. E., Lim, M. L., Reiner, J., Rote, W. E., Dempsey, E., Richard, B. M., Zhang, E., Tulinsky, A., Ripka, W. C., and Nutt, R. F. (1996) *J. Med. Chem. 39*, 4527−4530.
14. Bode, W., Turk, D., and Karshikov, A. (1992) *Protein Sci. 1*, 426−471.
15. Malikayil, J. A., Burkhart, J. P., Schreuder, H. A., Broersma, R. J., Jr., Tardif, C., Kutcher, L. W., III, Mehdi, S., Schatzman, G. L., Neises, B., and Peet, N. P. (1997) *Biochemistry 36*, 1034−1040.
16. Skrzypczak-Jankun, E., Rydel, T. J., Tulinsky, A., Fenton, J. W., II., and Mann, K. G. (1989) *J. Mol. Biol. 206*, 755−757.
17. Skrzypczak-Jankun, E., Carperos, V. E., Ravichandran, K. G., Tulinsky, A., Westbrook, M., and Maraganore, J. M. (1991) *J. Mol. Biol. 221*, 1379−1393.
18. Bartunik, H. D., Summers, L. J., and Bartsch, H. H. (1989) *J. Mol. Biol. 210*, 813−828.
19. Vijayalakshmi, J., Padmanabhan, K. P., Mann, K. G., and Tulinsky, A. (1994) *Protein Sci. 3*, 2254−2271.
20. Hendrickson, W. A. (1985) *Methods Enzymol. 115*, 252−270.
21. Finzel, B. C. (1987) *J. Appl. Crystallogr. 20*, 53−55.
22. DiCera, E., Guinto, E. R., Vindigni, A., Dang, Q. D., Ayala, Y. M., Meng, W., and Tulinsky, A. (1995) *J. Biol. Chem. 270*, 22089−22092.
23. Zhang, E., and Tulinsky, A. (1997) *Biophys. Chem. 63*, 185−200.
24. Hakansson, K., Tulinsky, A., Abelman, M. M., Miller, T. A., Vlasuk, G. P., Bergum, P. W., Lim-Wilby, M. S. L., and Brunck, T. K. (1995) *Bioorg. Med. Chem. 3*, 1009−1017.
25. Martin, P. D., Robertston, W., Turk, D., Huber, R., Bode, W., and Edwards, B. F. P. (1992) *J. Biol. Chem. 267*, 7911−7920.
26. Stubbs, M. T., Oschinkat, H., Mayr, I., Huber, R., Angliker, H., Stone, S. R., and Bode, W. (1992) *Eur. J. Biochem. 206*, 187−193.
27. Krishnan, R., Tulinsky, A., Vlasuk, G. P., Pearson, D., Vallar, P., Bergum, P., Brunck, T. K., and Ripka, W. C. (1996) *Protein Sci. 5*, 422−433.
28. Ganesh, V., Lee, A. Y., Clardy, J., and Tulinsky, A. (1996) *Protein Sci. 5*, 825−835.
29. Matthews, J. H., Krishnan, R., Costanzo, M. J., Maryanoff, R. E., and Tulinsky, A. (1996) *Biophys. J. 71*, 2830−2839.
30. Weber, P. C., Lee, S. L., Lewandowski, F. A., Schadt, M. C., Chang, C. H., and Kettner, C. A. (1994) *Biochemistry 34*, 3750−3757.
31. Geise, H. J., Buyr, H. R., and Mijlhoff, F. C. (1971) *J. Mol. Struct. 9*, 447−451.
32. Mathews, I. I., Padmanabhan, K. P., Ganesh, V., Tulinsky, A., Ishii, M., Chen, J., Turck, C. W., Coughlin, S. R., and Fenton, J. W., II (1994) *Biochemistry 33*, 3266−3279.
33. Morrison, J. F. (1982) *Trends Biochem. Sci. 7*, 102−105.
34. Schloss, J. V. (1988) *Acc. Chem. Res. 21*, 348−353.
35. Lewis, S. D., Lucas, B. J., Brady, S. F., Sisko, J. T., Cutrone, K. J., Sanderson, P. E., Freidinger, R. M., Mao, S.-S., and Gardell, S. J. (1998) *J. Biol. Chem. 273*, 4843−4854.
36. Schlechter, I., and Berger, A. (1967) *Biochem. Biophys. Res. Commun. 27*, 157−162.

BI980840E